Post-depositional subsidence of the Avellino tephra marker bed in the Pontine plain (Lazio, Italy)

van Gorp, W.; Sevink, J.; van Leusen, P. M.

Published in:
Catena

DOI:
10.1016/j.catena.2020.104770

Catena 194 (2020) 104770

Contents lists available at ScienceDirect

Catena

journal homepage: www.elsevier.com/locate/catena

Post-depositional subsidence of the Avellino tephra marker bed in the Pontine plain (Lazio, Italy): Implications for Early Bronze Age palaeogeographical, water level and relative sea level reconstruction

W. van Gorp[a,*], J. Sevink[b], P.M. van Leusen[a]

[a] Groningen Institute of Archaeology (GIA), University of Groningen, Groningen, the Netherlands
[b] Institute for Biodiversity and Ecosystem Dynamics (IBED), University of Amsterdam, Amsterdam, the Netherlands

ARTICLE INFO

Keywords:
Land subsidence
Soil ripening
Agro Pontino
Avellino tephra
Water level reconstruction
Relative Sea Level

ABSTRACT

Land subsidence has played and is still playing a significant role in coastal wetlands worldwide and in palaeogeographical reconstructions of such wetlands. The varying thickness of compaction-prone sediments over a stable subsurface is a key factor in determining its magnitude and in locating the most affected areas. In the coastal low-lying Agro Pontino (Lazio, Italy), subsidence of the past 90 years has been mapped using historical elevation data. Due to the fortunate preservation of distal Avellino tephra (AV-tephra, ca. 1900 cal. BCE) within its marshy strata, discovered a decade ago, detailed palaeogeographical reconstruction of the landscape in preparation for an assessment of its land use suitability in the Early Bronze Age (EBA) was possible. Current altitude variations of water-lain tephra in lake areas assumed to be connected necessitated a closer look at its original deposition altitude and the role of post-depositional subsidence. Recent subsidence patterns proved very useful for distinguishing stable from subsidence-prone areas. Two different EBA palaeo lake environments are distinguished: an inland and a near-coastal lake. The AV-tephra altitude variation within these lakes partly marks differential post-depositional subsidence within these lakes. Calculation of initial ripening of tephra-bearing lake deposits on top of shallowly buried Pleistocene ridges allowed for an estimation of original tephra deposition altitudes and associated lake levels. For the inland lake, a wide lake edge zone between 0.5 and 2 m above current sea level (m asl) was reconstructed, where EBA habitation or land use was possible. At the near-coastal lake, a water level of −1.5 to −1.3 m asl at the time of AV-tephra deposition was constrained. Because tephra deposition occurred here just after marine influence ceased, this altitude range is proposed to be a Relative Sea Level (RSL) index point at the time of AV-tephra deposition. The altitude range is in agreement with RSL models for tectonically stable areas in this region. The importance of subsidence in palaeogeographical, water level and RSL reconstructions in the region is stressed.

1. Introduction

Lowland coastal areas around the world often contain valuable depositional records of their Holocene evolution, which is determined by the interplay between Relative Sea Level (RSL) rise, climate change, alluvial processes and human activities. The role of compaction-driven subsidence of mainly peat and clay deposits is evident in many of these areas (e.g. Long et al., 2006). Sediment type and depth to an underlying non-compacting pre-Holocene or basement surface are main factors controlling such subsidence (Allen, 1999). Understanding land subsidence plays a key role in Holocene reconstructions of coastal basins, both in larger river deltas such as the Mississippi (Törnqvist et al., 2008; González and Törnqvist, 2009), the Rhine (Van Asselen et al., 2018; Erkens et al., 2016; Hijma and Cohen, 2019), the Tagus (Vis et al., 2008), the Po (e.g. Teatini et al., 2011; Fontana et al., 2017) and smaller deltaic and coastal back-barrier regions, such as in Southern England (Long et al., 2006; Massey et al., 2006) and several coastal basins along the Italian coast. Examples of the latter are the Arno plain (e.g. Rossi et al., 2011), the Sybaris plain in Calabria (e.g. Ferranti et al., 2011), and the Agro Pontino in Lazio (Serva and Brunamonte, 2007; van Gorp and Sevink, 2019), the last of which is the study area of this paper.

In most of these studies, the palaeogeographical reconstruction of coastal lagoons or back barrier areas with their coastal hinterland involves chronological controls in the form of radiocarbon dating of basal peats, which are the peats that form directly on top of the pre-Holocene

* Corresponding author.
E-mail address: W.van.Gorp@rug.nl (W. van Gorp).

https://doi.org/10.1016/j.catena.2020.104770
Received 27 January 2020; Received in revised form 24 June 2020; Accepted 26 June 2020
Available online 15 July 2020
0341-8162/

marine transgressional surface with rising groundwater level. With the slowing down of sea level rise around 6 ka BP (e.g. Lambeck et al., 2011) marine transgression ceased and coastal lagoons and back barrier regions containing wetland marshes were formed. The central parts of these areas were and still are prone to compaction-driven subsidence due to the thick peaty Holocene substrate. At the margins of these basins, where the underlying basement is near or at the current land surface, such autocompaction-driven subsidence is limited, and only compaction following drainage has occurred. This compaction through peat oxidation and physical ripening is irreversible (Zuur, 1958; De Bakker et al., 1990). Intensified reclamation of low-lying coastal areas in historical times but especially in the last century has caused increased subsidence rates in many areas around the world (e.g. van Asselen et al., 2018) and in many instances strongly modified the topography of the pre-reclamation land surface.

The recognition of a palaeo land surface in the sequence of coastal wetland deposits is not straightforward, because multiple environmental units are likely to co-exist in a complex spatial geometry. Detailed spatial analysis of palaeo records is needed to fully grasp the spatial complexity of such landscapes and their accompanying palaeo lake levels and RSL (Vis et al., 2015). This requires a thorough chronological control, which can usually be achieved only by means of extensive radiocarbon dating. However, a unique, both spatially and temporally sharply defined palaeogeographical 'window' can be reconstructed where distal tephra layers are regionally preserved within wetland deposits. This fortunate situation occurs in the coastal lowlands of the Agro Pontino and Fondi basin (Lazio, Central Italy), where the distal Avellino tephra (AV-tephra) marker bed (Monte Somma Vesuvius, ca. 1900 BCE; Alessandri, 2019) is preserved as a well-defined sandy tephra layer up to more than 1 cm thick in Holocene coastal wetland deposits (Sevink et al., 2011, Fig. 1).

The AV-tephra layer is well-preserved in the laminar clays, peats and calcareous gyttja (whitish lake marl deposits, e.g. Bakels et al., 2015) of the more tranquil lacustrine, marshy and shallow-water deposits, in which a fluvio-deltaic and two lake systems have been recognized (Van Gorp and Sevink, 2019). Its widespread presence created opportunities for detailed reconstruction of the central Italian Early Bronze Age (which is from now referred to as EBA) landscape which may serve as a context for a uniquely detailed model of EBA habitation and land use of fluvial and lake marginal zones. From recent reconstruction work by Van Gorp and Sevink (2019), post-depositional subsidence emerged as one of the factors to address in order to be able to reconstruct EBA palaeo lake-marsh levels and RSL based on AV-tephra altitude. The RSL is defined as the difference in altitude relative to the current mean sea level (asl) and given in 'm asl' in concordance with all other altitudes mentioned within this paper. Evidently, the current AV-tephra altitude and variations therein are the combined result of its initial altitude and post-depositional subsidence.

In this paper we present a study of the post-depositional subsidence of the AV-tephra (ca. 1900 BCE) using the relation between recent subsidence and depth to the underlying Pleistocene surface, and analysing different lake-marsh basins containing different sedimentary units. The specific aims are to better constrain EBA lake levels and lake edge zones in which the AV-tephra serves as a time marker, producing a reliable and detailed palaeogeographic reconstruction for the EBA. Additionally, using this reconstruction, an EBA RSL index point is obtained (ca. 1900 BCE).

2. Regional setting and background information

The Agro Pontino is located in Lazio, central Italy and consists of a coastal basin bordered by limestone mountains in the northeast and southeast, and by the Tyrrhenian Sea in the southwest (Fig. 1). It comprises a higher complex of Pleistocene marine terraces, Upper Pleistocene and Holocene beach ridges, and a lower-lying graben. This graben holds a major Holocene fill of lacustrine, marshy and fluvio/colluvial deposits (Fig. 1), largely covering earlier, Pleistocene marine terraces and beach ridges. The fluvial/colluvial infills mainly originate

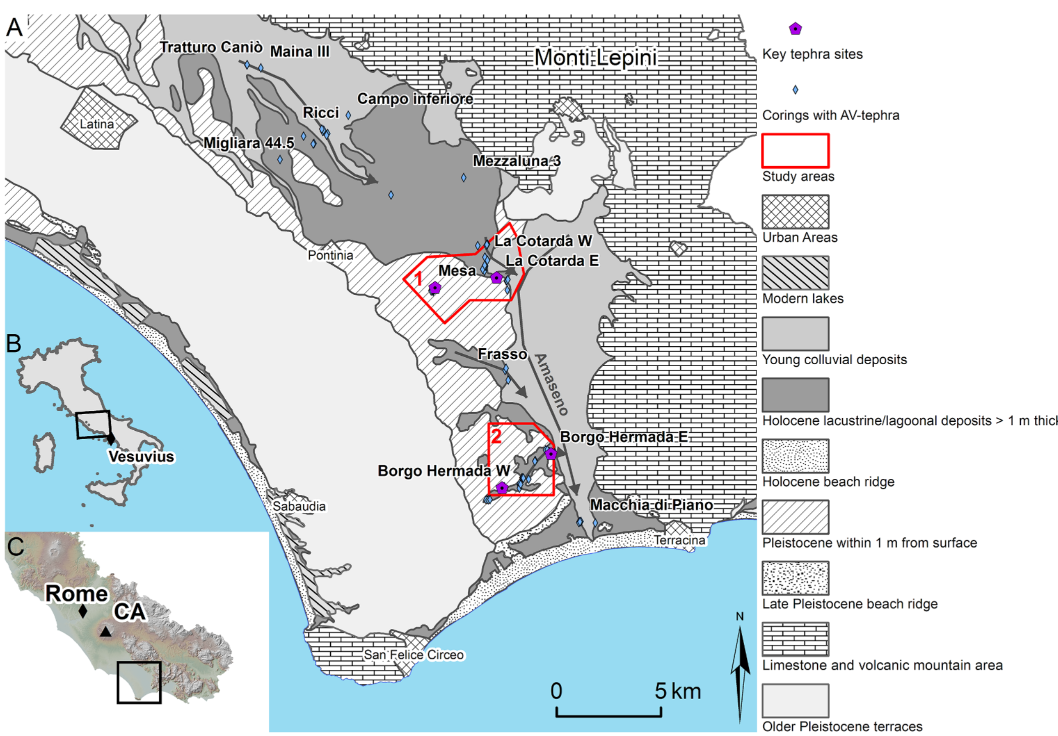

Fig. 1. A: Agro Pontino region with study areas, corings containing tephra and key tephra sites for this paper at Mesa-La Cotarda and Borgo Hermada indicated. The underlying Middle Holocene palaeogeography is based on Fig. 2 of van Gorp and Sevink (2019). The study area borders reflect the area for which the Pre-bonifica DEM has been checked and corrected. B: Italy with the location of the Vesuvius and the larger study region of C depicted. C: Larger study region, with the extent of map A depicted. CA = Colli Albani.

from discharge by rivers from the Colli Albani in the northwest and the Monti Lepini in the northeast and have partly covered the Holocene lagoonal and lacustrine deposits. Of these, the Amaseno River has produced most sediment (Fig. 1).

Reconstruction of the paleogeography around the time of AV-tephra deposition started in the northwestern part of the Agro Pontino basin, because the tephra layer was first discovered here. Since the EBA, this area evolved from a lacustrine environment fed by some small river systems to an area gradually infilled with fluvial, alluvial and colluvial sediments from the northwest. The adjacent central part became a peat marsh (Sevink et al., 2013). A later palaeoecological study of two sections containing the AV-tephra (Near Ricci and Mezzaluna, Fig. 1, Bakels et al., 2015) showed a wettening phase some time before deposition of the AV-tephra. A clear environmental change around the time of tephra deposition, either due to tephra deposition itself, or due to changed human activity, was not observed (Bakels et al., 2015). Bakels et al., (2015) also identified the presence of an EBA calcareous lacustrine zone in the northeast and a pyritic marsh along the southwestern border of this inland EBA lake.

Within the scope of the NWO-funded 'Avellino Event Project', a new landscape reconstruction study was carried out in the Agro Pontino (van Gorp and Sevink, 2019), including the southwestern part towards the outlet of the Amaseno River near the town of Terracina. The project aimed at the investigation of EBA settlement in the Agro Pontino, for which the AV-tephra could serve as a time marker (Sevink et al., 2011). This new study identified a separation between the aforementioned north-western inland lake system (referred to as 'inland lake') and a south-eastern near-coastal lake system made up of several infilled gully systems (referred to as: 'near-coastal lake'). The inland lake was blocked in the south by a shallow ridge formed by a Pleistocene marine terrace and in the north by the Amaseno alluvial fan which was building onto this Pleistocene ridge near La Cotarda (Fig. 1), effectively blocking the outlet and decoupling its lake level from direct influence of the sea. The near-coastal lake was formed by build-up of a coastal beach ridge and is marked by a sharp transition from lagoonal clays into brackish to freshwater peats and gyttjas (Van Gorp and Sevink, 2019). It was also noted that the altitude at which the AV-tephra was encountered varied within a single basin. A preliminary correlation between palaeogeographical units and recent land surface change (last 90 years) showed higher subsidence of areas where AV-tephra altitude is lower, suggesting that post-depositional subsidence of the AV-tephra layer might hamper detailed lake level and Relative Sea Level reconstruction (Van Gorp and Sevink, 2019).

The Agro Pontino has experienced surface elevation change in various ways. On the timescale of the Quaternary, tectonic warping and subsidence of the horst-graben system has both uplifted and buried old pre-MIS5 marine terraces (Sevink et al., 1982). In the Holocene, deformation due to tectonic activity has been marginal (Lambeck et al., 2004; Ferranti et al., 2006; Antonioli et al., 2009). At those locations where later burial by colluvial deposits did not take place, land surface altitude lowering of the Agro Pontino mainly occurred due to post-depositional subsidence of peaty and clayey sediments after drainage (Serva and Brunamonte, 2007). Autocompaction, including peat oxidation, and peat and clay ripening (e.g. Brain, 2015) are the main causes for this type of subsidence when the created accommodation space is not being filled by new sediments or peat build-up. In the Agro Pontino, land surface altitude increase occurred where younger colluvial and alluvial strata were built up on top of the lacustrine and lagoonal infillings (e.g. van Joolen, 2003; Feiken, 2014; summarized in Attema, 2017), and in these areas the buried EBA surface experienced compaction by weight. Since the EBA, land surface altitude change due to peat build-up and due to compaction has been controlled by fluctuating groundwater tables. Historically, the groundwater table has been artificially lowered several times, from the initial drainage of the Pontine Marshes during the Early Roman period through several phases of land management during the papal period, especially at the end of the 17th century CE. In the last century, subsidence has been massively enforced by a large-scale drainage program carried out in the 1930s (Grande Bonifica Integrale; e.g. Serva and Brunamonte, 2007). However, this recent subsidence shows a large spatial variation and the altitude of some areas has hardly been affected by these recent land management activities (Van Gorp and Sevink, 2019).

Another factor controlling the amount of subsidence is the depth of the stable underlying surface. In the Agro Pontino, this surface consists of Pleistocene beach ridge deposits and marine terraces formed during marine high stands in the Upper Pleistocene. These deposits have not only experienced tectonic movements during the Upper Pleistocene but have also been fluvially dissected in especially MIS 2 (e.g. Sevink et al., 2018), when sea level was at a low point of −125 m asl during the Last Glacial Maximum (Lambeck et al., 2014). This dissected Pleistocene landscape is therefore present as an undulating palaeosurface above, at, or below current sea level, with sometimes deep incisions. As a consequence, the remaining non-eroded Pleistocene soils at or near the current land surface have experienced at least 80 ka of compaction, ripening and other soil forming processes prior to their flooding in connection with the Holocene sea level rise, as discussed in Sevink et al. (2018). Holocene subsidence of these fully ripened Pleistocene sediments, which are easily distinguishable from the plastic, humic to peaty unripe Holocene clays, thus is negligible, in contrast to areas with deep Holocene fills. The subsidence pattern of the last 90 years seems to confirm this (Van Gorp and Sevink, 2019).

In summary, these previous studies indicated that land surface subsidence is larger in areas with thick Holocene deposits, but the subsidence of the AV-tephra layer itself, and thus of the accompanying EBA land surface, remained unknown.

3. Methods

3.1. Study areas

Two areas have been chosen to investigate post AV-tephra subsidence and water level reconstruction as they are crucial in understanding the Mid to Late Holocene development of the entire Agro Pontino (Van Gorp and Sevink, 2019). Each area represents a closed lacustrine unit, within which a single lake level is assumed to have existed at the time of AV-tephra deposition. They differ with respect to their water level and the nature of their Holocene fill. Study area 1, at Mesa-La Cotarda (Fig. 1), is part of the southern edge of the inland Agro Pontino lacustrine region, including its now buried main drainage outlet. At the western (Mesa) and south-eastern (La Cotarda East) edges, which are key tephra sites within this study, the Pleistocene surface is present within one meter from the surface and is overlain by shallow Holocene clayey and peaty deposits. AV-tephra is present in the top 50 cm and underlain by a thin peat layer. La Cotarda is located at the eastern edge of the inland lake and its lake level should therefore be similar to that of Mesa. AV-tephra is present in a thin cover of Holocene pyritic clays on top of the Pleistocene surface and in a thick peaty fill of the inland lake. The eastern part of La Cotarda is covered by post-Bronze Age sediment originating from the Amaseno river (e.g. Van Joolen, 2003, pp. 70–84).

Study area 2 is situated around the town of Borgo Hermada (Fig. 1), in the near-coastal south-eastern part of the Agro Pontino. It contains a Pleistocene gully infilled with a sequence of Holocene brackish marine clays containing lagoonal bivalves of *Cerastoderma glaucum.* At the edges of this gully, where the Pleistocene subsurface rises up, layers of broken shells occur. On top of these lagoonal deposits, calcareous gyttja and finally peats occur. AV-tephra is encountered at varying depth. Throughout the infilled gully, the tephra is located within a few dm above the transition from brackish marine clays to calcareous gyttja. At its former eastern outlet into the palaeo-Amaseno (Borgo Hermada E, key tephra site Fig. 1), the AV-tephra is almost continuously present in calcareous gyttja overlain by a thick peat deposit (Fig. 2). Its depth and

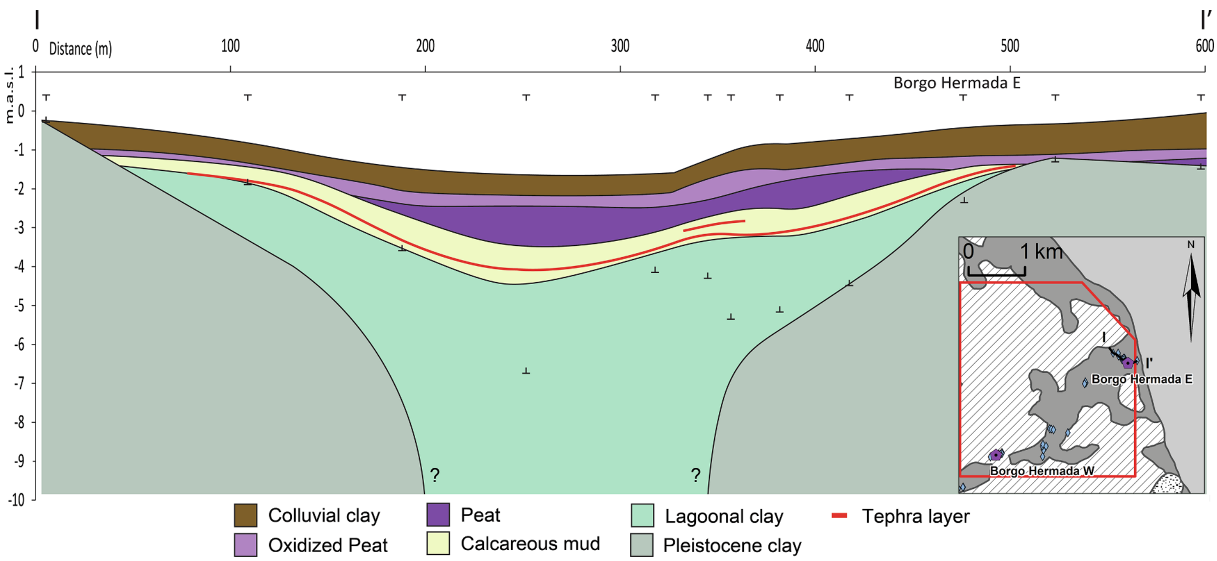

Fig. 2. Cross section I-I′ across the Borgo Ermada gully, near its outlet into the Amaseno valley. Brown: fluvio-colluvial and brought-up clay, light purple: oxidized peat, purple: peat, yellow: gyttja, green: marine clays. Tephra layers in red. Inset shows the map of Fig. 1 with the location of the cross section.

altitude vary in relation to its position within the gully cross-section. A few dm above the AV-tephra in the gyttja, a second, younger tephra layer is occasionally encountered (Fig. 2) that has been identified as AP2 – a younger eruption originating from the Monte Somma Vesuvius (Sevink et al., unpublished results). In its western upslope area (Borgo Hermada W, key tephra site in Fig. 1), AV-tephra is present within peats, often just above the transition from a marine to a marshy environment (Van Gorp and Sevink, 2019). Palaeo-ecological analyses of some of these settings as well as geochemical analyses of tephra and radiocarbon datings of enclosing peats will be presented in separate forthcoming papers.

3.2. General workflow

Before presenting the detailed methodologies, the general workflow is described. New coring data were obtained using Edelman hand cores or gauge corings of which soil characteristics as well as lithological and lithostratigraphical information were collected. First, to obtain the best spatially explicit picture of the thickness of the Holocene deposits, all available coring data was combined to generate a Pleistocene subsurface model. Second, recent subsidence was estimated by subtracting a recent LiDAR-based digital elevation model (Ministero dell'Ambiente e della Tutela del Territorio e del Mare, www.pcn.minambiente.it) from a similar but historic model based on the 1:5000 scale topographical map series created in 1928–1932 by the Italian Military Geographic Institute (IGMI) in preparation for the major land reclamation of the 1930s. The results are checked using the two study areas introduced in Section 3.1, which play a key role in understanding lake reconstruction. Altitudes of the pre-Bonifica and the current surface, the tephra altitude, and the top of the Pleistocene surface as derived from individual corings are analyzed to understand their correlation. To generate a reliable estimate of EBA water levels, two representative corings from each study area are selected, in each of which a shallow Holocene cover rests on top of a stable Pleistocene subsurface. This limited thickness of the Holocene cover ensures a low uncertainty in the calculated amount of compaction. Post-depositional ripening of the soil layers within the selected corings since the deposition of AV-tephra was calculated using three scenarios based on different assumptions about soil characteristics, which will be explained in detail below. These calculations were compared to observed post-1928 subsidence and current AV-tephra altitude within lake edge areas with a shallow stable Pleistocene subsurface. Results for the two study areas and general implications for EBA palaeo lake evolution and Relative Sea Level reconstruction are then discussed.

3.3. Pleistocene subsurface model

Cores documenting the depth of the Pleistocene surface and thicknesses of overlying lithologies were selected from Sevink et al. (1984), van Joolen (2003), Feiken (2014), Barbieri et al. (1999), Eisner and Kamermans (2004), and Serva and Brunamonte (2007) and from hand coring data collected for the Avellino Event project. Areas with stable Pleistocene deposits at the surface were separated from those with Holocene deposits at the surface and were clipped from the modern LiDAR DEM, which was resampled from its original resolution of 2 × 2 m to 10 × 10 m. The Holocene deposits were subdivided into sandy beach ridge deposits, young colluvial deposits, and wet, low lying lagoonal, marshy and lacustrine deposits; the latter being most susceptible to compaction.

Based on the earlier and recent soil data, part of the Holocene area was then classified as having Pleistocene deposits within one meter from the surface. Finally, the approximate locations of the main Pleistocene valley axis draining the inland Agro Pontino lake and those of the smaller gully systems discharging into the palaeo-Amaseno River in the near-coastal lake area were determined. A palaeo-Amaseno drained into the Mediterranean towards a base level determined by the low sea level during the Last Glacial Maximum. Because the exact location of this Pleistocene valley floor is not known, it is placed in the centre of the current Amaseno Valley, using the current Pre-Holocene surfaces as valley walls. The topo-to-raster module of ArcGIS 10.3 (ESRI, 2014) was used to produce the interpolated Pleistocene surface (Fig. 3). Inputs used included coring data, the area with Pleistocene at shallow depth, palaeo-rivers and a zero-depth contour for the edge of the current Pleistocene surface. Especially in areas with Pleistocene at shallow depth, for which more data is available, a detailed image is obtained. Because data is scarce in the deepest parts of the inland Agro Pontino and in the Amaseno river basin, the interpolated surface is a gross estimate of Pleistocene depth in these areas. However, the DEM was checked to ensure that, at least, it agreed with information from deep corings that did not reach the Pleistocene subsurface.

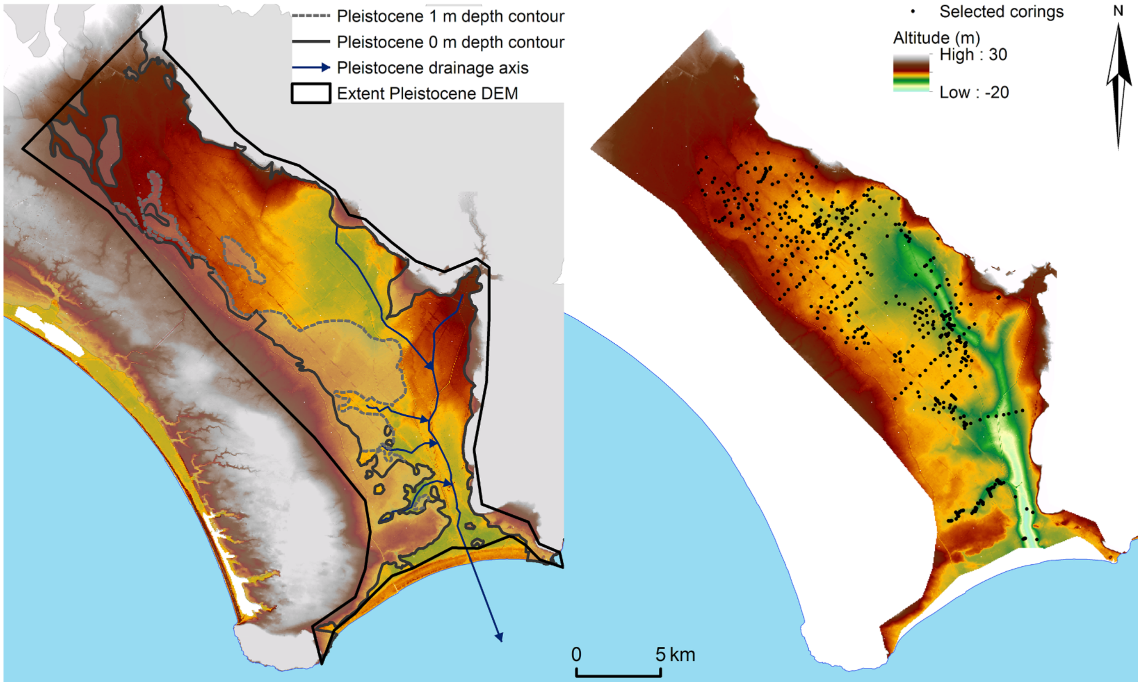

Fig. 3. Left: inputs used for Pleistocene surface reconstruction on top of the LiDAR DEM (Ministero dell'Ambiente e della Tutela del Territorio e del Mare). Shaded area depicts area with Pleistocene at or within 1 m from the surface, bordered by their respective contours. Right: reconstructed Pleistocene surface. Grid size = 50 × 50 m. Altitude scale is the same for both maps. Selected corings contain points from Sevink et al. (1984), Van Joolen (2003), Feiken (2014), and van Gorp and Sevink (2019).

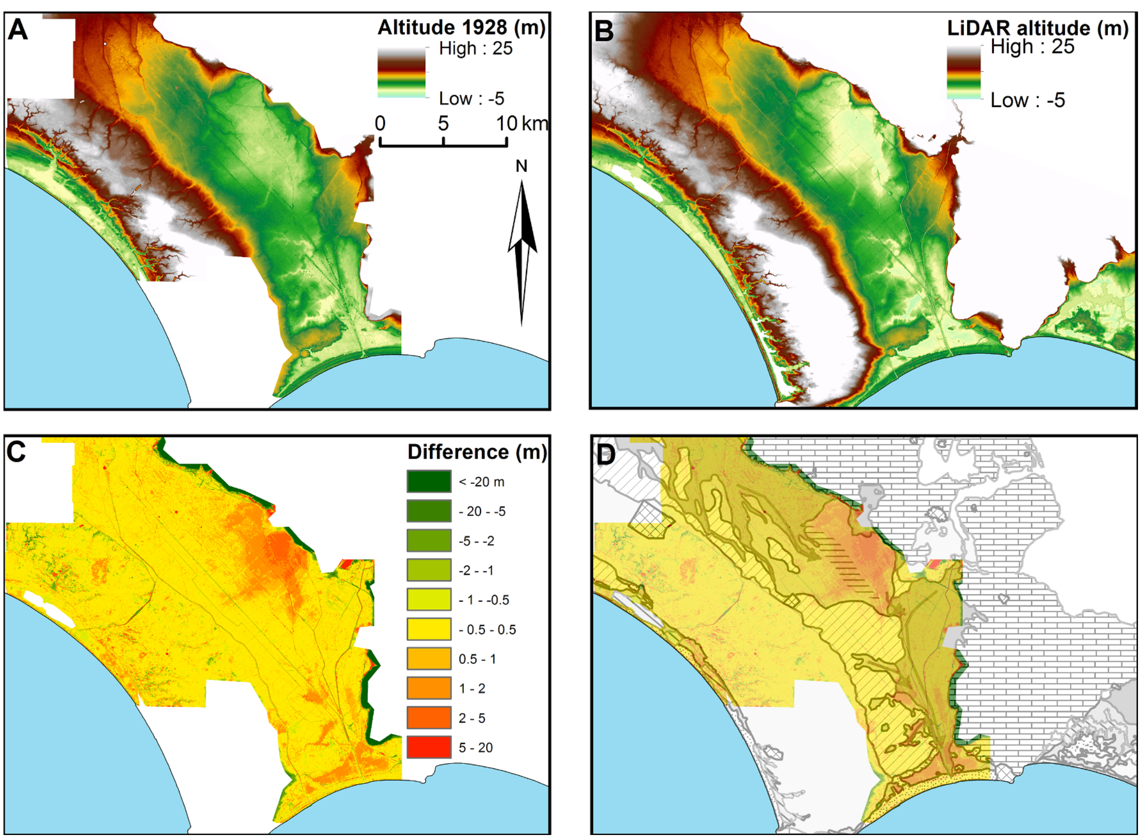

Fig. 4. A: 1928 DEM based on 1926-1932 1:5000 IGMI topographic map series, B: LiDAR image. C: Difference between map A and map B. D: map C overlain with geographical units of Fig. 1. Based on Fig. 5 from van Gorp and Sevink (2019), see Fig. 1 for unit legend.

3.4. Pre-1928 DEM reconstruction

A preliminary comparison of modern surface altitudes with those from before the Grande Bonifica Integrale of the 1930s reveals recent subsidence patterns that visually correlate with Holocene depositional units (Fig. 4, van Gorp and Sevink, 2019). The following, more careful, reconstruction of the historical altitudes is based on the 1926–1932 1:5000 IGMI (Italian Geographic Military Institute) topographic map series, made for the reclamation of the Pontine plain and published by the Consorzio della Bonifica di Piscinara (we obtained black-and-white scans of copies of these sheets held in the State Archive at Latina). On average, each of the 149 sheets contains about 75 contour lines (spaced 0.5 m apart) and 1800 surveyed elevation points, which have been digitised and interpolated to a raster elevation model with 10 m-sized cells. The elevation data were digitised at the precision provided by the source – i.e. to the nearest dm in nearly all cases, as less than 1% of the elevation points were measured to a precision of 1 cm.

The corners of the original map sheets have geographic coordinates using the Roma Monte Mario datum, but with an unstated projection. Using a shapefile of the sheet boundaries originally provided by the Regione Lazio in Gauss Boaga-Monte Mario Rome II, we georeferenced the scanned sheets by their corners to ED1950-UTM33N, leaving unaltered any internal deformations caused by the scanning or already present in the hardcopy versions (Baiocchi et al., 2019).

When comparing the georeferenced sheets with more recent, and therefore presumably more accurate, publicly available geodata – specifically the 1 m resolution 2010 LiDAR DEM, the 1:10,000 Carta Technica Regionale topographic map of 1990, and the 1:5000 cadastral map of 2002 (IGM) – we noted horizontal deviations of between 5 and 20 m. Since not enough information was available about the original datum and projection of the Bonifica map series, and further distortions might have been caused by various stages of copying and scanning, manually shifting the historical DEM by 16.5 m to the North and 11.5 m to the West could only reduce the maximum horizontal error to about 10 m. The effect of this shift on land surface altitude is less than 0.2 m for most of the study area, with larger differences limited to artificial features such as roads and canals. Subsidence was then calculated as the difference between the 1928 (Bonifica) and 2010 (LiDAR) altitudes.

A further slight correction was then applied, based on the assumption that surfaces directly on the Pleistocene substrate would not have subsided significantly since 1928. Any calculated subsidence for such areas must have been due to a systematic difference in the vertical datum used for the 1928 and 2010 DEMs, or to a systematic and widespread surface lowering due to agricultural activities, or to both at the same time. For the stable locations of Study areas 1 and 2 (Fig. 1), the 2010 LiDAR DEM altitude turns out to be systematically 0.2 m lower than that of the 1928 DEM. To avoid overestimation of total subsidence by compaction and drainage, this altitude difference has been subtracted from measured subsidence values in the following analysis.

3.5. Subsidence analysis

Recent surface and AV-tephra layer subsidence were analyzed by comparing AV-tephra altitudes in individual corings within the same lake unit and relating them to the thickness of Holocene sediments as derived from the Pleistocene subsurface model. Tephra altitudes from individual corings within the inland palaeo-lake were analysed separately from those within the near-coastal palaeo-lake. Only corings containing a well-described AV-tephra layer were used. For study area 1 (the inland lake) a subdivision between the lake centre (calcareous gyttja), the west-northwestern lake edge near Mesa (peat and pyritic clay) and the lake edge-outlet area near La Cotarda (peat and pyritic clay) is made. For study area 2 (the near-coastal lake north of the town of Borgo Hermada) a subdivision between lake centre (gyttja) and lake edge (peat) corings is made.

We estimated soil shrinkage by calculating physical ripening of the soil since drainage. Physical ripening can be used to calculate volume loss of clayey soils due to water drainage and has been empirically described for Dutch clayey soils in the ripening formula of Zuur (1958), Eq. (1). To optimize EBA water level estimation of locations where AV-tephra has been encountered in shallow water deposits, minimum, mid, and maximum ripening scenarios were calculated for typical soils in the two study areas. Only soils with a shallow Holocene cover on top of a stable Pleistocene subsurface, where compaction of deeper layers can be ruled out, were eligible. For these thin (< 1 m) Holocene deposits on top of a stable Pleistocene subsurface, the ripening formula of Zuur (1958) is sufficient to estimate the amount of surface and tephra layer subsidence, while for thicker Holocene deposits the constraint on the necessary soil parameters is too weak to be reliably calculated. The soil physical ripening formula is empirically described and estimates the amount of compaction a soil has endured since initial drainage:

$$Wsat1 = n(fL + b * fh) + C\,[-] \tag{1}$$

where

$Wsat1$ = Mass fraction water/solid phase ('water number') [–]
n = Ripening factor [–]
fL = Mass fraction lutum (< 2 μm) [–]
fh = Mass fraction organic matter [–]
b = 3, Water binding capacity of organic matter vs lutum [–]
C = 0.2, Constant [–]

Following the approach described in De Bakker et al. (1990) it is possible to calculate original soil thickness by calculating its shrinkage. This is done by relating the water number of the current soil with that of the initial soil. First, the water number of the current soil layer is calculated using the massic volume, which is the volume of moist soil under field conditions divided by the mass of dried soil, and thus the reciprocal of the dry bulk density of soil. Shrinkage, or vertical lowering of the soil layer can then be calculated by relating the two water numbers. The formulas (A.1)–(A.6) describing these steps are given in Appendix A.

Because soil parameters such as soil bulk density and organic matter fraction have not been measured, we used three scenarios to estimate the right order of magnitude of these parameters, based on representative soil properties from Sevink et al. (1984, pp. 107–109, Appendix B). Within these scenarios two parameters are varied: (1) mass fraction of organic matter fh is varied to be between 0.02 and 0.75, depending on soil material, and (2) massic volume of the current soil has been estimated using typical values for clay soils from the Netherlands, mostly ranging between 0.63 and 0.83, coinciding with bulk densities of between 1.6 and 1.2 kg/dm^3 (De Bakker et al., 1990). We have translated these variations into three scenarios for each soil, estimating a min, mid, and max scenario for soil ripening (Appendix B).

In study area 1, the south-eastern border of the inland lake, soils at the key tephra sites at La Cotarda East and Mesa have a shallow Holocene pyritic clay cover on top of the Pleistocene substrate. In study area 2, the near-coastal lake near Borgo Hermada, two key tephra sites containing shallow Holocene deposits of different composition have been compared. The first, Borgo Hermada W, consists almost entirely of clayey peat, peat and lagoonal clay. The second, Borgo Hermada E, contains shallow lagoonal clays, gyttja, and a younger clay deposit. It is acknowledged that in peaty soils, peat compaction and oxidation of the upper part after drainage is significant and we address this by varying the organic matter fraction in this soil between 0.25 and 0.75 (Appendix B). Assumptions have been made about organic matter density using an averaged value from Erkens et al. (2016) for Dutch peats of 0.103 kg/dm^3 ranging from 0.08 to 0.150 kg/dm^3. Because variation along this range has a marginal effect on the soil shrinkage calculated, we have only used the average value. The effect of varying

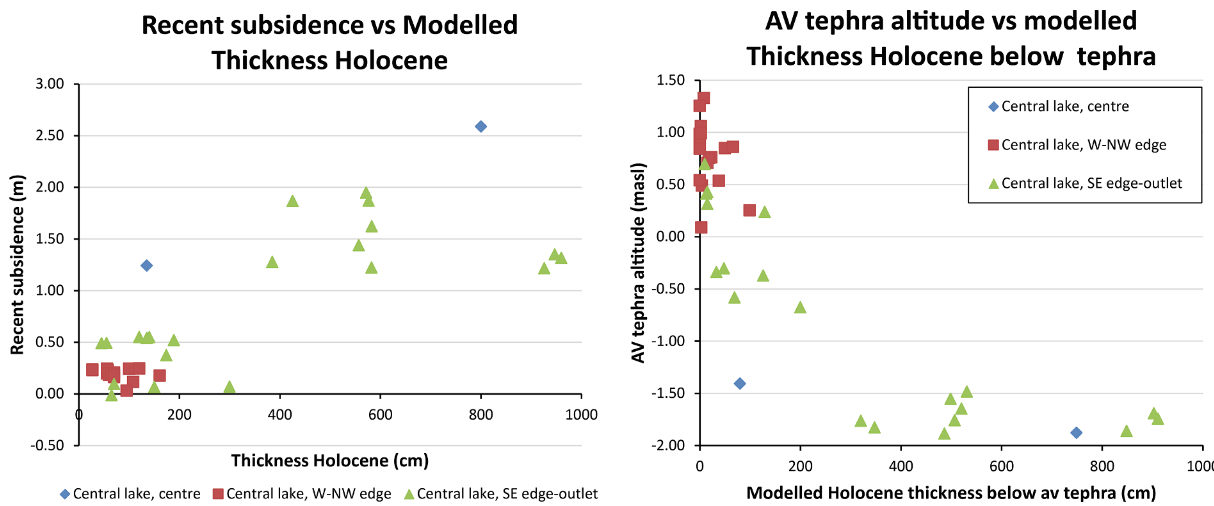

Fig. 5. Inland lake. A: Recent land surface subsidence in relation to Holocene thickness and B: AV-tephra altitude in relation to underlying modelled thickness of Holocene below tephra.

organic matter fraction and massic volume is larger, and therefore these parameters are varied within the three scenarios. Their contribution to modelled subsidence will be addressed in the discussion Section 5.

4. Results

4.1. Subsidence of different lake zones

Individual coring data of the relevant landscape units show the patterns of land subsidence and AV-tephra altitude in relation to the underlying Holocene thickness (Fig. 5). In study area 1, the inland lake, an increase of subsidence with increasing modelled Holocene thickness can be observed, whilst a concomitant decrease of tephra altitude can be seen with increasing thickness of *underlying* Holocene deposits. The W-NW lake edge is located in an area with low subsidence, corresponding to low thickness of Holocene deposits. Dots in the lake centre represent tephra observed in calcareous gyttja, indicating open water (e.g. Bakels et al., 2015). Within study area 1, the SE edge outlet dots (green triangles) represent corings in peat, peaty clay, and pyritic clay. Here large variations in AV-tephra depth and a clear correlation with Holocene thickness and recent subsidence are observed. In fact, two groups may be observed, distinguished by small Holocene thickness and low subsidence vs large Holocene thickness and high subsidence (Fig. 5A), respectively. Fig. 5B shows a similar division, with a decreasing trend of tephra altitude with Holocene modelled thicknesses below tephra until at least 2 m of these modelled thicknesses. For thicknesses of 4 m and higher, a fluctuating but rather constant tephra altitude around −1.5 to −2 m asl can be observed. Since the recent subsidence running up to 2 m cannot entirely account for the altitude difference between the highest and lowest tephra deposits in the SE lake edge area, original lake bottom altitude difference and/or pre-1928 subsidence induced by earlier land use (see Section 2) accounts for this difference.

Altitudes in study area 2, the near-coastal lake, paint a slightly different picture. Subsidence does not clearly increase with increasing Holocene thickness. Subsidence of peats and gyttja both show a wide variation (Fig. 6). Peats show a generally declining AV-tephra altitude with increasing Holocene thickness, but tephra-bearing peats only occur in the distal part of the gully. The largest Holocene thicknesses correspond with corings in calcareous gyttja, which generally are present in the deeper and wider downstream reach of the original Pleistocene gully. The five largest Holocene thicknesses in both graphs of Fig. 6 correspond to the coastal basin and not to the Borgo Hermada gully. These data points form a separate group that will be discussed in Section 5.1.

4.2. Compaction (ripening) calculation results

For each study area, two corings have been chosen to calculate surface and tephra layer subsidence. For the inland lake edge area (study area 1), one of the two selected locations, at La Cotarda (Fig. 7), represents shallow water in the margins of the outlet of the inland lake. The second selected location, at Mesa, represents the inland lake edge. Calculated land surface subsidence varies between 0.34 and 1.75 m at these inland lake edge locations of study area 1. This variation is driven by the chosen range for organic matter content, whose fractions range from < 0.02 to 0.20 in clay soils, and massic volume of the clay, ranging from 0.63 to 0.83 (See Appendix B). Subsidence of the AV-tephra layer is, however, < 0.5 m in every scenario, and AV-tephra altitudes in both locations are consistently around 0.5–0.6 m asl (Table 1, Fig. 7).

In Study area 2, the near-coastal lake, two locations with a different lithologies show different compaction (Table 1, Fig. 7). Site Borgo Hermada E contains tephra in calcareous gyttja, which experienced limited compaction, whereas Borgo Hermada W contains tephra within a thicker Holocene fill that is mostly composed of peats and therefore more prone to compaction. Current tephra altitude is therefore lower in the peats. It is unlikely that surface altitude at the time of AV-tephra deposition was lower at the peaty site than at the gyttja site. Thus, subsidence caused by peat compaction must have caused this lower tephra altitude. The mid and max scenarios of Borgo Hermada E result in tephra altitudes equal to or higher than those at Borgo Hermada W, which results in a lake level range between −1.5 and −1.3 m asl that will be discussed in Section 5.4.

5. Discussion

The relation between subsidence and coastal Holocene infillings deposited in backwaters, lagoons or marshy areas is well recognized in coastal and deltaic regions worldwide (e.g. Carminati and Martinelli, 2002; Törnqvist et al., 2008; Van Asselen et al., 2009; Erkens et al., 2016). In Italy, examples from Holocene coastal regions demonstrate the impact of subsidence on current lowland altitudes (e.g. Brunetti et al., 1998; Marra et al., 2013) and configurations (Rossi et al., 2011). In the Agro Pontino, Serva and Brunamonte (2007) identified the impact of subsidence by shrinkage and compaction. Our work confirms this subsidence for the inland part of the Agro Pontino (Van Gorp and Sevink, 2019) and demonstrates how its magnitude depends on the depth of the Pleistocene subsurface and lithology of the Holocene sediments. The presence of a shallow (< 1 m depth) Pleistocene subsurface limits recent and future subsidence, whereas the inland and near-

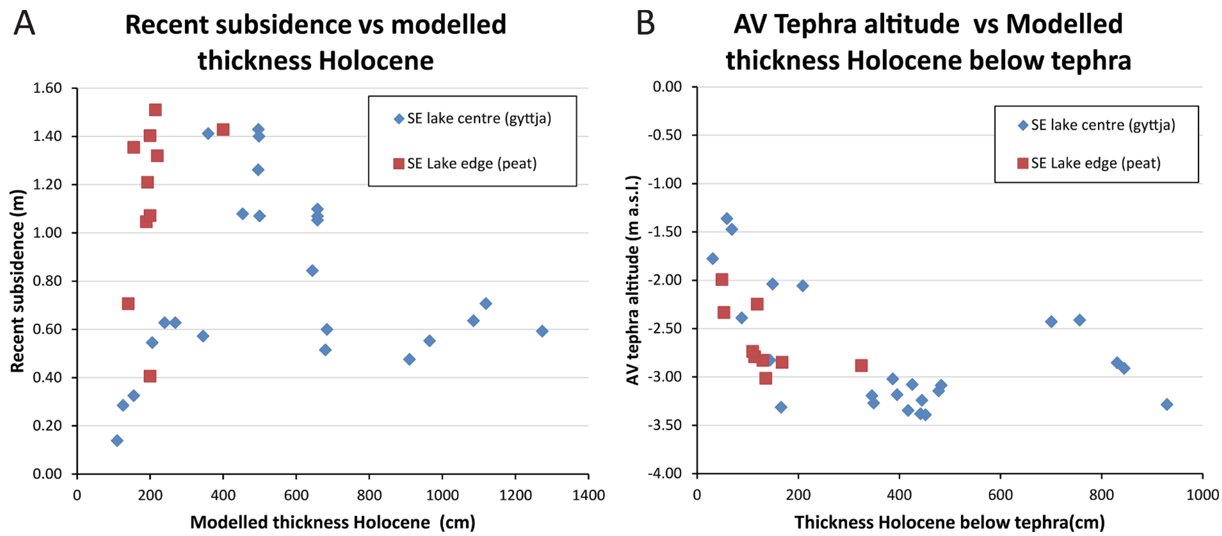

Fig. 6. Near-coastal lake. A: Recent land surface subsidence in relation to Holocene thickness B: and tephra altitude in relation to underlying Holocene thickness of study area 2.

coastal locations with thick Holocene clays and peats will likely continue to subside as a result of peat oxidation due to lowering of the water table and further compaction by weight of deeper unconsolidated sediments (e.g. Van Asselen et al., 2018).

Locations where the Pleistocene subsurface is present at a shallow depth, and the amount of subsidence has therefore been limited, sometimes coincide with lake edges where the AV-tephra is present in laminated pyritic clays. These clays form in very shallow, tranquil, and anoxic backwaters that have become pyritic due to water coming from sulfuric karstic springs at the foot of the Monti Lepini and other northern sources, and their origin and weathering have extensively been discussed recently by Sevink (2020). AV-tephra altitude is highest in the northern part of the inland lake and slowly decreases via the western lake edge (including Mesa) towards the inland lake outlet area at La Cotarda. This corresponds with a decreasing Pleistocene subsurface altitude and represents a small NW-SE gradient from distal floodplain to marshy deposits. AV-tephra altitude in the centre of the lake is, however, significantly lower, as has already been indicated in van Gorp and Sevink (2019), and this corresponds to thicker underlying compaction-prone Holocene deposits. The tephra altitude within the corings of the western edges of the inland lake varies by up to one meter, which may be explained by variation in the original lake bottom altitudes or by differences in the peat/clay ratio of strata underlying the tephra, leading to different compaction rates.

5.1. Measurement and process uncertainties

Besides the modelled subsidence, the observed variation in tephra altitudes reflects uncertainties in (1) altitude measurement, (2) initial lake bottom altitudes, and (3) rates of post-depositional subsidence. Whilst altitude measurement uncertainties may account for up to 0.2 m of variation, they do not explain observed systematic differences within the different inland lake zones, or the large variation in altitudes across the lake zones in the near-coastal lake. Such differences and variations

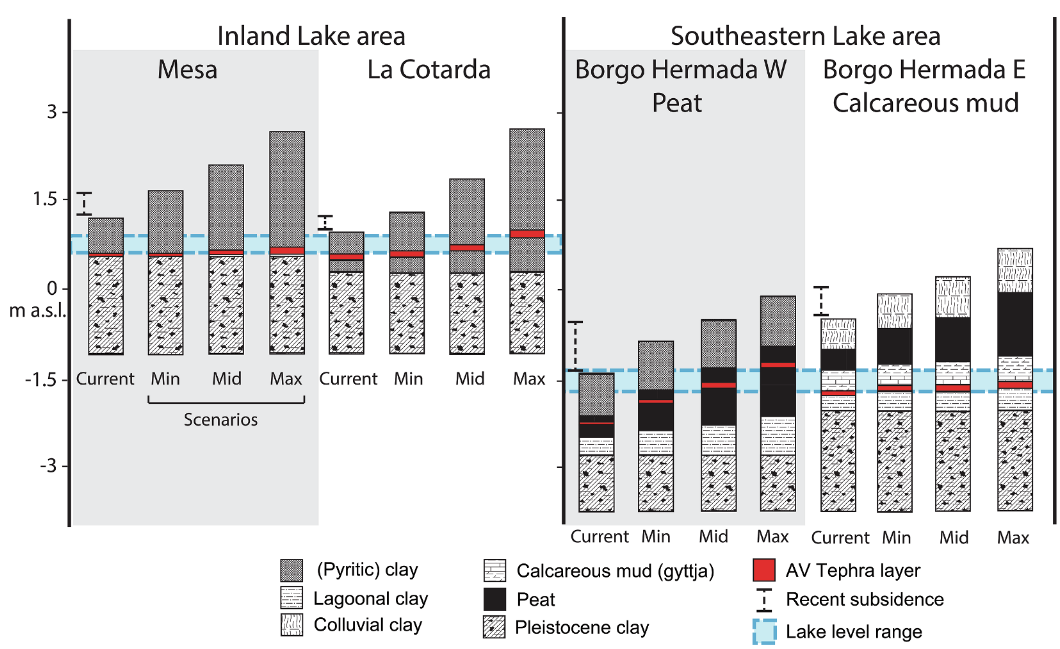

Fig 7. Calculated Subsidence scenarios (min, mid, max) compared for four selected soils in the two study areas. Current profile, recent subsidence since 1928 and water level reconstruction are also shown.

Table 1
Altitudes of land surface (top), AV-Tephra layer and Pleistocene subsurface top for the actual situation and according to the three (min, mid, max) ripening scenarios.

Coring	Mesa 504				Cotarda E 399				BH 301				BH 331			
	Lon	Lat			Lon	Lat			Lon	Lat			Lon	Lat		
	13.0998	41.4040			13.1396	41.3997			13.1730	41.3240			13.1460	41.3092		
m asl	Actual	min	mid	max	Actual	min	mid	max	Actual	min	mid	max	actual	min	mid	max
Top	1.2	1.6	2.1	2.6	0.9	1.3	1.8	2.7	−0.5	−0.1	0.2	0.7	−1.5	−0.9	−0.6	−0.2
Tephra	0.6	0.6	0.6	0.6	0.5	0.6	0.7	0.9	−1.8	−1.7	−1.7	−1.6	−2.3	−1.9	−1.6	−1.3
Pleist	0.6	0.6	0.6	0.6	0.3	0.3	0.3	0.3	−2.1	−2.1	−2.1	−2.1	−2.9	−2.9	−2.9	−2.9

thus have to be explained by lake-bottom depth (deposition altitude) and post-depositional subsidence. This is illustrated by the AV tephra altitude in study area 2 (Borgo Hermada; Fig. 6), where the five data points with the largest Holocene thickness below the tephra layer display somewhat deviating AV-tephra altitudes. This may be caused by their location directly adjacent to the coast at Macchia di Piano (Fig. 1). Here, an underlying sandier substrate likely is present, corresponding to the Holocene beach ridge that was building up with the slowing down of sea level rise. Although no such deposits were reached by these corings, removing these five data points reveals more clearly the general trend of decreasing tephra altitude with increasing Holocene thickness.

For locations with shallow Holocene deposits underlain by a stable Pleistocene subsurface, where ripening can be considered a better estimate for its subsidence, calculated land subsidence ranges are large due to uncertainties in material properties. The unavailability of measured bulk densities and organic matter fractions is the reason we used three subsidence scenarios in which massic volume and organic matter fraction have been varied (Fig. 7). For example, peat oxidation above the groundwater table can significantly contribute to subsidence. The significance of these differences for subsidence reconstruction must be explained within the context of each specific area, as discussed in Sections 5.2–5.4.

5.2. Tephra subsidence at the inland lake edge

The measured recent land surface subsidence of around 2 m in the inland lake area is reflected in the difference in tephra altitude between the lake centre and edges. However, untangling original lake depth, ripening, oxidation and self-weight compaction is difficult. For the central part of the lake, the occurrence of tephra in both peats and gyttjas at a rather consistent altitude of −1.5 to −2 m suggests that both environments have undergone subsidence. The gyttja thickness at, for example, Mezzaluna is only 50 cm and it is enclosed by peat. Subsidence by compaction of the underlying peat will thus probably have been similar to those locations where tephra is directly enclosed in thick layers of peat. The compaction of peat overlying tephra has been substantial as well. In the central parts of the lake, the many corings containing a 0.5–1 m thick oxidized peat layer overlying the tephra show that this process is an important contributing factor to the observed recent subsidence, as also indicated by Serva and Brunamonte (2007).

For the lake edge zone, where recent subsidence is limited, the calculated ripening for Mesa and La Cotarda East shows that compaction of the pyritic clays led to significant land subsidence, but only limited subsidence of the AV-tephra layer incorporated within these clays (Fig. 7). Because La Cotarda is located at or near the lake outlet, its original tephra altitude should be similar to or less than that at Mesa. This implies that the amount of subsidence at La Cotarda East should not be higher than indicated by the mid-scenario, which predicts an original tephra altitude of ca. 0.6 m asl.

5.3. Lake edge reconstruction of the EBA inland lake (study area 1)

The reconstruction of the Pleistocene subsurface altitudes, combined with the occurrence of the AV-tephra layer in shallow water deposits

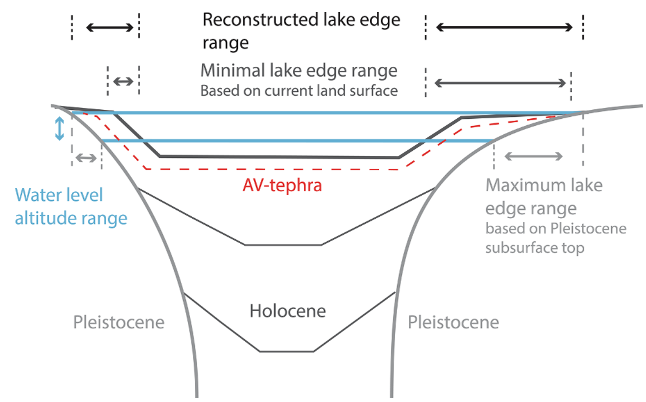

Fig. 8. Conceptual diagram of altitude-based lake edge reconstruction. Lake edge zones are defined within altitude ranges derived from tephra altitude and lake depth reconstruction.

directly on top of Pleistocene deposits, provides an opportunity to reconstruct the EBA lake edge zone. We define this zone as the altitude-based spatial range within which the transition from the subaerial landscape on the Pleistocene ridge to the lake occurs (Fig. 8). In places, this excludes peaty areas that may be located within the central part of the lake. The averaged reconstructed altitudes of AV-tephra in study area 1 follow a decreasing NW-SE trend from around 2 m asl at the northern lake edge to around 0.5 m asl at the outlet area of La Cotarda. This leads to a very gentle gradient of around 0.025%, whilst the gradient between Mesa and La Cotarda in the southwestern lake edge area is negligible. Because the tephra was deposited in a very shallow anoxic environment, lake level altitude for the outlet area is confined to 0.5–1 m asl (Fig. 7). However, for the lake area as a whole, the wider altitude range of 0.5–2 m asl is more applicable for lake edge reconstruction. As the underlying Pleistocene surface would determine the maximum extent of the lake if no Holocene sediments were present, selecting the area defined by this altitude range from the underlying Pleistocene surface leads to a spatial range in which the maximum lake extent at the time of AV-tephra deposition can be expected (Figs. 8 and 9).

In the subsiding areas that are not overlain by younger colluvial deposits, selecting the area defined by same altitude range (0.5–2 m asl) from the current LiDAR surface, provides an area for the minimum lake extent. This is valid as altitude within this spatial range dips towards the lake centre, while tephra depth is consistently within 1 m from the surface in the inland lake. Both ranges combined then form a robust spatial constraint of the EBA inland lake edge (Figs. 8 and 9). This significantly improves lake edge zones estimated solely on the basis of soil map units (Feiken, 2014; Van Gorp et al., 2017) and therefore provides a more solid basis for future prospection for EBA settlement and land use evidence (Fig. 9). The gentle gradient of the Pleistocene subsurface leads to a spatially wide lake edge zone in the northwestern and the southern lake edges which largely coincide with the sedimentary units in which the AV-tephra has been encountered. Note that in the northwest, the lake edge zone overlaps with floodplain units which slightly slope up out of the lake edge zone. For instance, Migliara 44.5 is located outside the lake edge zone but tephra does occur within pyritic

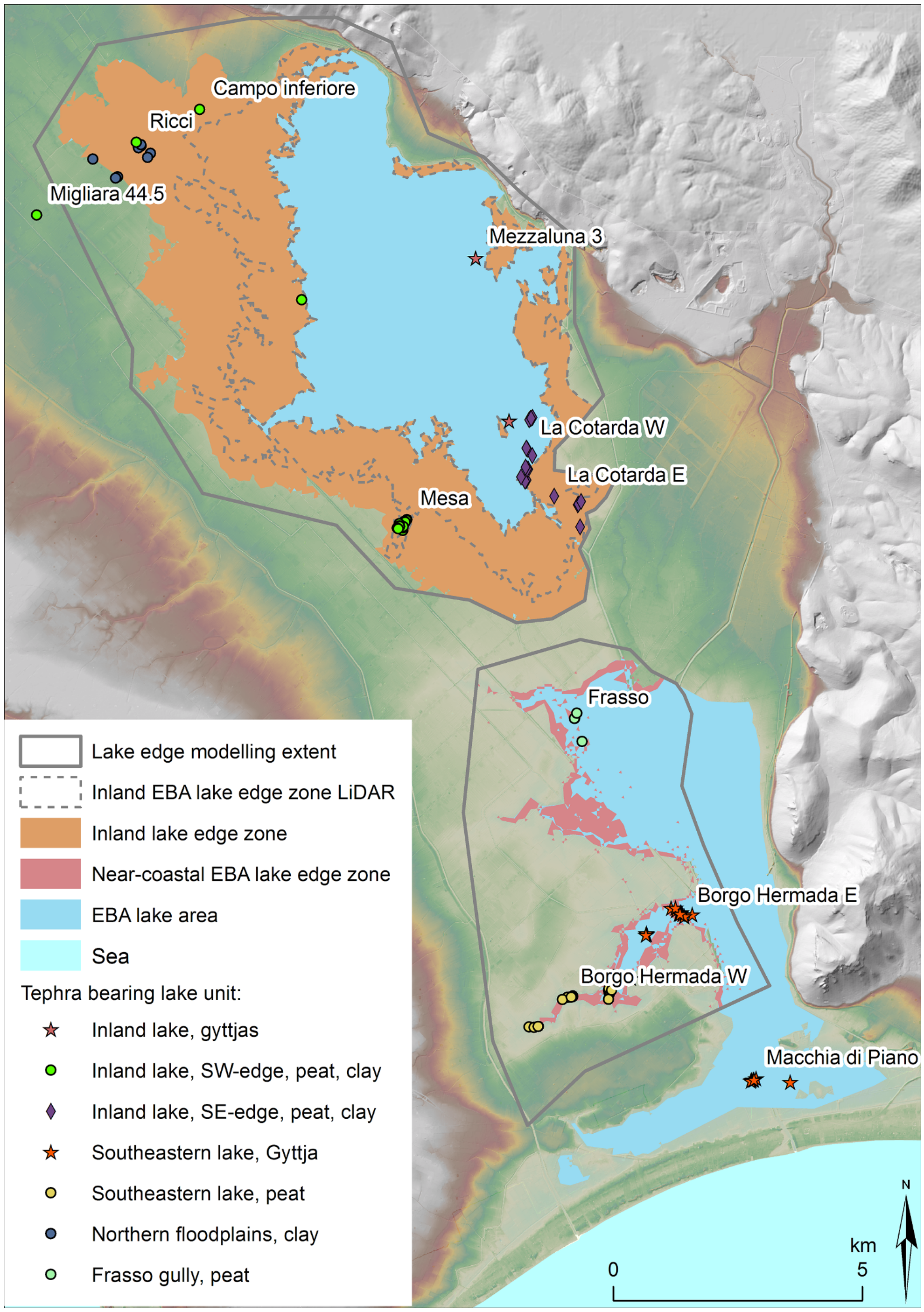

Fig. 9. Lake edge reconstruction following the method displayed in Fig. 8 and using a margin of +0.5 to 2 m asl for the inland lake and a margin of −2 to −1 m asl for the near-coastal lake based on Pleistocene depth reconstruction and current LiDAR altitude. The maximum EBA lake extent is based on the Pleistocene subsurface DEM. For the near-coastal lake, lake edge zones are modelled for a smaller extent due to uncertain data for the eastern and southern area. Background shows current LiDAR altitude.

clay (Sevink et al., 2011). This may be due to the presence of lacustrine zones at higher altitude within a complex flood basin architecture.

5.4. Lake edge reconstruction of the EBA near-coastal lake (Study area 2, Borgo Hermada)

For study area 2, the calculated original tephra altitudes range between −2 and −1 m asl for lake marginal zones. Selecting the spatial extent of this altitude range from the modelled Pleistocene subsurface top again leads to a maximum lake edge range, in the same way as for study area 1. In this case, however, due to the steep Pleistocene valley walls, resulting lake edge ranges are much narrower than for the inland lake (Fig. 9). Additionally, due to the presence of younger colluvial sediments in the northern and eastern part of the EBA near-coastal palaeolake and an evolving Holocene beach ridge at the Southern edge, only the eastern lake edge can be reconstructed with sufficient confidence.

It is clear that the infill history of the near-coastal lake differs somewhat from that of the inland lake. It shows a diachronic terrestrialisation pattern since marine influence ceased at around 2000 BCE,

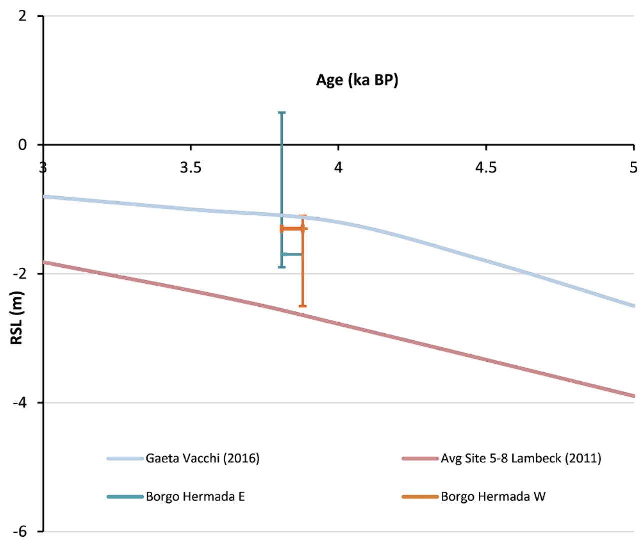

Fig. 10. Sea level upper and lower boundaries compared to Relative Sea Level curves from Lambeck et al. (2011) and Vacchi et al. (2016).

in which lake edges are formed by marshes (peat) and the lake centre is open water (calcareous gyttja) at the time of the AV-tephra deposition. This open water is later overgrown by marsh vegetation (Cross section Fig. 2). The AV-tephra is thus found in peats at the lake edges and in gyttja at the lake centre. However, the current AV-tephra altitude variation within and between these sedimentary units appears unrelated to the division between lake edge and lake centre (Fig. 5). The lake edges do not always coincide with the presence of the top of a gently sloping Pleistocene ridge closely underneath the AV-tephra layer. Locally, this caused tephra-bearing peat deposits at the EBA lake edge to subside more than the gyttjas in the lake centre. Only in the deepest part of the lake, towards its connection with the Amaseno basin, is the tephra found at very low altitudes: below −3 m asl. As this forms the central part of the lake, the water here may have been deeper. Additionally, thick Holocene deposits that are experiencing ongoing compaction by weight here underlie the AV-tephra.

However, within this former outlet area of the infilled Borgo Hermada gully, tephra-bearing gyttja is also found on top of the Pleistocene ridge at Borgo Hermada East, where it is much thinner and located at a higher altitude (Fig. 7). Here subsidence of the tephra layer has been minimal, and we can therefore obtain a good estimate for the original lake bottom depth at around −1.7 m asl. The thickness of the water column above the gyttja cannot be determined; it can range from a few dm to one or two meters. Besides subsidence, this range could account for much of the water-lain tephra altitude variation in the lake cross section as shown in Fig. 2. If we assume a minimum water column of 0.2 m and a maximum of 1 m, a lake level of −1.5 to −0.7 m asl is obtained. In addition, the tephra within peats at the Borgo Ermada West site shows a maximum reconstructed altitude of −1.3 m asl (Fig. 7, Table 1) and may serve as a maximum water level (terrestrial) limiting point (e.g. Vacchi et al., 2016). The combination of Borgo Hermada East and West brackets the lake level to −1.5 to −1.3 m asl.

The wider altitude range of between −2 to −1 m used to reconstruct the lake edge zone (Fig. 8) still results in a narrow lake edge zone. Since we have a relatively high degree of confidence in the position of the EBA lake edge, we can use theoretical models of EBA settlement and land use behaviour to target areas for archaeological surface and coring prospection. The upstream part of the infilled Borgo Hermada gully contains a known Middle Bronze Age archaeological site postdating the AV-tephra deposition (e.g. Alessandri, 2016), but no indications of EBA settlements have been found so far. Additionally, the low-lying region between Frasso and Borgo Hermada may be a candidate for further local palaeogeographical exploration within the scope of suitable EBA lake margins where the AV tephra is present as a time marker, as it falls within the modelled lake edge zone (Fig. 9). Although tephra has been found at a few locations, observational Pleistocene subsurface data of that region is mostly absent.

5.5. Implications for near-coastal lake level and Relative Sea level

In the near-coastal lake, the AV-tephra was deposited in a lacustrine environment just after the diminishing of marine influences in this area (Fig. 2; Van Gorp and Sevink, 2019). This potentially links AV-tephra altitude to the contemporary sea level. Different models of Relative Sea Level Rise have been applied to the area (e.g. Lambeck et al., 2011; Vacchi et al., 2016) and the AV-tephra may serve as an excellent marker if local factors such as post-depositional subsidence can be quantified.

The near-coastal lake and marsh deposits show a fast shift from brackish-marine to brackish-freshwater environments and likely mark beach ridge closure at the Amaseno outlet, occurring just before AV-tephra deposition. The reconstructed lake water level therefore serves as a good indication for the contemporary sea level. Because the selected locations for lake level reconstruction (Fig. 9) are on top of the stable Pleistocene surface, the tephra-bearing strata barely suffered post-depositional compaction or subsidence and can be regarded as basal peats or lake sediments (e.g. Van de Plassche et al., 2010; González and Törnqvist, 2009; Fontana et al., 2017; Hijma and Cohen, 2019). The reconstructed near-coastal lake level of −1.5 to −1.3 m asl is therefore also a best estimate of local Relative Sea Level, fitting well with the recent standardization of Sea Level indicators around the Mediterranean (Vacchi et al., 2016). The fortunate preservation of tephra at the transition from a marine to a freshwater environment is a uniquely useful marker in this sense.

The two main modelled EBA Relative Sea Levels for the region differ due to different isostatic models (Lambeck et al., 2011, 2004; Antonioli et al., 2009; Vacchi et al., 2016). Local variability occurs due to Late Pleistocene extensional tectonics and graben formation, but the now exposed Pleistocene marine terraces in which the Borgo Ermada gully has been formed are tectonically stable since MIS 5 (Ferranti et al., 2006). The scenario-based modelling of initial compaction after land falls dry demonstrates its use for the reconstruction of the original depositional altitude. Altitudes of marshy deposits, assumed to be stable and used as sea level markers, may in fact have experienced significant compaction, leading to an underestimation of Relative Sea Level (e.g. Vacchi et al., 2016). Our reconstructed EBA Relative Sea Level at the time of the Avellino eruption (ca. 1900 Cal BCE; Alessandri, 2019) is ca. 1 m higher than modelled in regional curves 5–8 of Lambeck et al. (2011), but in line with those presented by Vacchi et al. (2016) for the Gulf of Gaeta (Fig. 10).

5.6. Archaeological implications

Subsidence of Late Holocene sediments implies subsidence of any entrained archaeological features and materials – a process highly relevant to our understanding of the formation and preservation of these archives as well as the palaeogeographical context in which they were formed. Like many other European coastal low-lying areas that changed from a subaqueous to a subaerial environment during the Late Holocene, the Agro Pontino contains traces of prehistoric human settlement and land use (Alessandri, 2016). Unfortunately, the majority of the evidence tends to be buried under more recent sediments, becoming available for study only occasionally when soils are more deeply excavated for construction projects. The Early to Middle Bronze Age settlement density and human impact on the landscape are therefore still poorly understood, even if palaeoecological data indicate limited human activity (e.g. Bakels et al., 2015; Doorenbosch and Field, 2019). Our reconstruction of the lake boundary zones represents a step towards the palaeogeographical reconstruction of the Early to Middle Bronze Age landscape of the Agro Pontino, and thus to a more refined land suitability model (Van Joolen, 2003) that will guide future, more systematic, archaeological prospection.

6. Conclusions

The observed altitude variation of the AV-tephra marker bed in the Agro Pontino is caused by three palaeogeographical factors: (1) the initial gradient of the fluvio-deltaic and lacustrine systems, (2) the initial lake bottom depth of lacustrine and lagoonal units, and (3) post depositional subsidence, both in historic and in recent times. Elevation changes derived from cartographic data of 1928 pinpoint areas that have experienced significant, and likely ongoing, recent land subsidence. Palaeogeographical analysis has allowed us to select locations that experienced limited recent subsidence, hence suitable for the reconstruction of post-AV-tephra deposition subsidence. Subsidence at these locations was modelled to reconstruct EBA lake levels, providing both a constraint on local sea level (ca. −1.3 to −1.5 m asl) and guidance for the planning of future archaeological prospection of the EBA landscape. Our sea level range is in line with recent RSL models of the tectonically stable areas in the central Tyrrhenian area. Palaeogeographical and subsidence reconstruction was vital for the establishment of this palaeo lake level and RSL index point. Our study confirms the importance of both management-related subsidence and autocompaction in palaeogeographical reconstructions of Middle Holocene coastal wetland environments in the central Mediterranean. In the Agro Pontino this is particularly important for studies on early (prehistoric) land suitability, and water level or RSL reconstruction.

Funding

This work was supported by The Netherlands Organisation for Scientific Research (NWO) Free Competition grant 360-61-060.

Declaration of Competing Interest

The authors declare that they have no known competing financial interests or personal relationships that could have appeared to influence the work reported in this paper.

Acknowledgements

The authors wish to thank all members of the Avellino Event project team and all students that participated in fieldwork in the period 2015–2017. We further wish to express our gratitude to the anonymous reviewers of this article, for their helpfull comments. Corings at the site of Mesa were done in cooperation with Gijs Tol of the University of Melbourne and Tymon de Haas of Leiden University.

Appendix A. Supplementary material

Supplementary data to this article can be found online at https://doi.org/10.1016/j.catena.2020.104770.

References

Alessandri, L., 2016. Hierarchical and federative polities in protohistoric Latium Vetus. An analysis of Bronze Age and Early Iron Age settlement organization. In: Attema, P. A.J., Seubers, J., Willemsen, S. (Eds.), Early States, Territories and Settlements in Protohistoric Central Italy. University of Groningen/Groningen Institute of Archaeology & Barkhuis, Groningen, pp. 67–82.

Alessandri, L., 2019. The early and Middle Bronze Age (1/2) in South and central Tyrrhenian Italy and their connections with the Avellino eruption: An overview. Quatern. Int.

Allen, J.R.L., 1999. Geological impacts on coastal wetland landscapes: some general effects of sediment autocompaction in the Holocene of northwest Europe. The Holocene 9, 1–12.

Antonioli, F., Ferranti, L., Fontana, A., Amorosi, A., Bondesan, A., Braitenberg, C., Dutton, A., Fontolan, G., Furlani, S., Lambeck, K., Mastronuzzi, G., Monaco, C., Spada, G., Stocchi, P., 2009. Holocene relative sea-level changes and vertical movements along the Italian and Istrian coastlines. Quatern. Int. 206, 102–133.

Attema, P., 2017. Sedimentation as geomorphological bias and indicator of agricultural (un)sustainability in the study of the coastal plains of South and Central Italy in antiquity. J. Archaeolog. Sci.: Rep.

Baiocchi, V., Alessandri, L., Giannone, F., Sevink, J., van Gorp, W., van Leusen, P.M., 2019. Pre-Pre-Bonifica maps of the Agro Pontino: an assessment. Proceedings 2018 IEEE International Conference on Metrology for Archaeology and Cultural Heritage, October 2018, Cassino, Italy.

Bakels, C., Sevink, J., Kuijper, W., Kamermans, H., 2015. The Agro Pontino region, refuge after the Early Bronze Age Avellino eruption of Mount Vesuvius, Italy? Analecta Praehistorica Leidensia 45, 55–68.

Barbieri, M., Carrara, C., Castorina, F., Dai Pra, G., Esu, D., Gliozzi, E., Paganin, G., Sadori, L., 1999. Multidisciplinary study of Middle-Upper Pleistocene deposits in a core from the Piana Pontina (central Italy). Giorn. Geol. 47–73.

Brain, M.J., 2015. Compaction. Handbook of Sea-Level Research. John Wiley & Sons, Ltd, Chichester, UK, pp. 452–469.

Brunetti, A., Denèfle, M., Fontugne, M., Hatté, C., Pirazzoli, P.A., 1998. Sea-level and subsidence data from a Late Holocene back-barrier lagoon (Valle Standiana, Ravenna, Italy). Mar. Geol. 150, 29–37.

Carminati, E., Martinelli, G., 2002. Subsidence rates in the Po Plain, northern Italy: the relative impact of natural and anthropogenic causation. Eng. Geol. 66, 241–255.

De Bakker, H., Locher, W.P., Steur, G.G.L., 1990. Bodemkunde van Nederland, Deel 2: Bodemgeografie. Malmberg, Den Bosch, pp. 250–256.

Doorenbosch, M., Field, M.H., 2019. A Bronze Age palaeoenvironmental reconstruction from the Fondi basin, southern Lazio, central Italy. Quatern. Int. 499, 221–230.

Eisner, W., Kamermans, H., 2004. Late Quaternary vegetation history of Latina, Italy: a final report on the Mezzaluna core. In: Holstrom, S., Voorrips, A., Kamermans, H. (Eds.), The Agro Pontino Archaeological Survey. Archaeological Studies Leiden University (ASLU) 11, Leiden.

Erkens, G., van der Meulen, M.J., Middelkoop, H., 2016. Double trouble: subsidence and CO2 respiration due to 1,000 years of Dutch coastal peatlands cultivation. Hydrogeol. J. 24, 551–568.

ESRI, 2014. ArcGIS 10.3. Redlands, USA.

Feiken, H., 2014. Dealing with Biases, Three Geo-archaeological Approaches to the Hidden Landscapes of Italy. PhD thesis. University of Groningen.

Ferranti, L., Antonioli, F., Mauz, B., Amorosi, A., Dai Pra, G., Mastronuzzi, G., Monaco, C., Orrù, P., Pappalardo, M., Radtke, U., Renda, P., Romano, P., Sansò, P., Verrubbi, V., 2006. Markers of the last interglacial sea-level high stand along the coast of Italy: Tectonic implications. Quatern. Int. 145–146, 30–54.

Ferranti, L., Pagliarulo, R., Antonioli, F., Randisi, A., 2011. "Punishment for the Sinner": Holocene episodic subsidence and steady tectonic motion at ancient Sybaris (Calabria, southern Italy). Quatern. Int. 232, 56–70.

Fontana, A., Vinci, G., Tasca, G., Mozzi, P., Vacchi, M., Bivi, G., Salvador, S., Rossato, S., Antonioli, F., Asioli, A., Bresolin, M., Di Mario, F., Hajdas, I., 2017. Lagoonal settlements and relative sea level during Bronze Age in Northern Adriatic: Geoarchaeological evidence and paleogeographic constraints. Quatern. Int. 439, 17–36.

González, J.L., Törnqvist, T.E., 2009. A new Late Holocene sea-level record from the Mississippi Delta: evidence for a climate/sea level connection? Quat. Sci. Rev. 28, 1737–1749.

Hijma, M.P., Cohen, K.M., 2019. Holocene sea-level database for the Rhine-Meuse Delta, The Netherlands: Implications for the pre-8.2 ka sea-level jump. Quat. Sci. Rev. 214, 68–86.

Lambeck, K., Antonioli, F., Purcell, A., Silenzi, S., 2004. Sea-level change along the Italian coast for the past 10,000 yr. Quat. Sci. Rev. 23, 1567–1598.

Lambeck, K., Antonioli, F., Anzidei, M., Ferranti, L., Leoni, G., Scicchitano, G., Silenzi, S., 2011. Sea level change along the Italian coast during the Holocene and projections for the future. Quatern. Int. 232, 250–257.

Lambeck, K., Rouby, H., Purcell, A., Sun, Y., Sambridge, M., 2014. Sea level and global ice volumes from the Last Glacial Maximum to the Holocene. Proc. Natl. Acad. Sci. 111, 15296–15303.

Long, A.J., Waller, M.P., Stupples, P., 2006. Driving mechanisms of coastal change: Peat compaction and the destruction of late Holocene coastal wetlands. Mar. Geol. 225, 63–84.

Marra, F., Bozzano, F., Cinti, F.R., 2013. Chronostratigraphic and lithologic features of the Tiber River sediments (Rome, Italy): Implications on the post-glacial sea-level rise and Holocene climate. Global Planet. Change 107, 157–176.

Massey, A.C., Paul, M.A., Gehrels, W.R., Charman, D.J., 2006. Autocompaction in Holocene coastal back-barrier sediments from south Devon, southwest England, UK. Mar. Geol. 226, 225–241.

Rossi, V., Amorosi, A., Sarti, G., Potenza, M., 2011. Influence of inherited topography on the Holocene sedimentary evolution of coastal systems: An example from Arno coastal plain (Tuscany, Italy). Geomorphology 135, 117–128.

Serva, L., Brunamonte, F., 2007. Subsidence in the Pontina Plain, Italy. Bull. Eng. Geol. Environ. 66, 125–134.

Sevink, J., Vos, P., Westerhoff, W., Stierman, A., Kamermans, H., 1982. A sequence of marine terraces near Latina (Agro Pontino, Central Italy). Catena 9, 361–378.

Sevink, J., Remmelzwaal, A., Spaargaren, O., 1984. The Soils of Southern Lazio and Adjacent Campania. Publicaties van het Fysisch-Geografisch en Bodemkundig Laboratorium van de Universiteit van Amsterdam 38, Amsterdam.

Sevink, J., van Bergen, M.J., van der Plicht, J., Feiken, H., Anastasia, C., Huizinga, A., 2011. Robust date for the Bronze Age Avellino eruption (Somma-Vesuvius): 3945 ± 10 calBP (1995 ± 10 calBC). Quat. Sci. Rev. 30, 1035–1046.

Sevink, J., van der Plicht, J., Feiken, H., van Leusen, P.M., Bakels, C.C., 2013. The Holocene of the Agro Pontino graben: Recent advances in its palaeogeography,

palaeoecology, and tephrostratigraphy. Quatern. Int. 303, 153–162.
Sevink, J., 2020. Burnt clay or terra bruciata in coastal basins of Southern Lazio, Italy: Evidence for prehistoric ignicoltura or resulting from drainage of Holocene pyritic sediments? J. Archaeolog. Sci.: Rep. 32, 102432.
Sevink, J., Di Vito, M., Piochi, M., Mormone, A., van Gorp, W., Bakels, C., 2018. A rare Mid-Würmian lithoid tuff in the Agro Pontino graben (Southern Lazio, Italy) and its identification as an Albano 5–7 related distal tephra deposit (41–36 kaBP): characteristics, provenance and palaeogeographical implications. Ann. Geophys. 61.
Sevink, J., van Gorp, W., Di Vito, M.A., Arienzo, I., submitted for publication. Mid-Late Holocene distal tephra in the Agro Pontino and Fondi basin (Southern Lazio, Italy): occurrence, origin and revised age (unpublished results).
Teatini, P., Tosi, L., Strozzi, T., 2011. Quantitative evidence that compaction of Holocene sediments drives the present land subsidence of the Po Delta, Italy. J. Geophys. Res. 116.
Törnqvist, T.E., Wallace, D.J., Storms, J.E.A., Wallinga, J., van Dam, R.L., Blaauw, M., Derksen, M.S., Klerks, C.J.W., Meijneken, C., Snijders, E.M.A., 2008. Mississippi Delta subsidence primarily caused by compaction of Holocene strata. Nat. Geosci. 1, 173.
Vacchi, M., Marriner, N., Morhange, C., Spada, G., Fontana, A., Rovere, A., 2016. Multiproxy assessment of Holocene relative sea-level changes in the western Mediterranean: Sea-level variability and improvements in the definition of the isostatic signal. Earth Sci. Rev. 155, 172–197.
van Asselen, S., Stouthamer, E., van Asch, T.W.J., 2009. Effects of peat compaction on delta evolution: A review on processes, responses, measuring and modeling. Earth Sci. Rev. 92, 35–51.
van Asselen, S., Erkens, G., Stouthamer, E., Woolderink, H.A.G., Geeraert, R.E.E., Hefting, M.M., 2018. The relative contribution of peat compaction and oxidation to subsidence in built-up areas in the Rhine-Meuse delta, The Netherlands. Sci. Total Environ. 636, 177–191.
van de Plassche, O., Makaske, B., Hoek, W.Z., Konert, M., van der Plicht, J., 2010. Mid-Holocene water-level changes in the lower Rhine-Meuse delta (western Netherlands): implications for the reconstruction of relative mean sea-level rise, palaeoriver-gradients and coastal evolution. Netherlands J. Geosci. – Geologie en Mijnbouw 89, 3–20.
van Gorp, W., Alessandri, L., Doorenbosch, M., 2017. De kustbekkens van Zuid-Lazio in de Vroege Bronstijd ten tijde van de Avellino-eruptie (Somma-Vesuvius): een welkome plek of een vijandige omgeving? Tijdschrift voor Mediterrane Archeologie 57, 10–16.
van Gorp, W., Sevink, J., 2019. Distal deposits of the Avellino eruption as a marker for the detailed reconstruction of the Early Bronze Age depositional environment in the Agro Pontino and Fondi Basin (Lazio, Italy). Quatern. Int. 499, 245–257.
van Joolen, E., 2003. Archaeological Land Evaluation. A Reconstruction of the Suitability of Ancient Landscapes for Various Land Uses in Italy Focused on the First Millennium BC. PhD thesis. University of Groningen, Groningen.
Vis, G., Cohen, K.M., Westerhoff, W.E., Veen, J.H.T., Hijma, M.P., van der Spek, Ad, JF, Vos, P.C., 2015. Paleogeography. In: Handbook of Sea-Level Research. John Wiley & Sons, Chichester, UK, pp. 514–535.
Vis, G., Kasse, C., Vandenberghe, J., 2008. Late Pleistocene and Holocene palaeogeography of the Lower Tagus Valley (Portugal): effects of relative sea level, valley morphology and sediment supply. Quat. Sci. Rev. 27, 1682–1709.
Zuur, A., 1958. Bodemkunde der nederlandse bedijkingen en droogmakerijen, deel C: Het watergehalte, de indroging en enkele daarmee samenhangende processen. Directie Wieringermeer/Landbouwhogeschool, Wageningen.